Authors final submitted manuscript.
Puublished as: J. Mass Spectrom. v. 37 p. 1131-1140 (2002)
DOI 10.1002/jms.374
URL: http://onlinelibrary.wiley.com/doi/10.1002/jms.374/abstract

Ionization Energy Reductions in Small 2,5-Dihdroxybenzoic Acid / Proline Clusters

Gary R. Kinsel,[1*] Richard Knochenmuss,[2] Patrick Setz,[2] C. Mark Land,[1] Sor-Koon Goh,[1] Edet F. Archibong,[1] Jon H. Hardesty[1] and Dennis S. Marynick[1]

[1]Department of Chemistry and Biochemistry, University of Texas at Arlington, 502 Yates Street, Arlington, TX 76019-0065.

[2]Laboratorium für Organische Chemie, Eidgenössiche Technische Hochschule, Universitättstr. 16, CH-8092 Zürich, Switzerland.

*To whom correspondence should be addressed. E-mail: kinsel@uta.edu

Phone: 817-272-3541

FAX: 817-272-3808

Running Title: **IE Reductions in 2,5-DHB / Proline Clusters**

Text: 19, Figures: 8, Tables: 2

Abstract

The photoionization of $(pro)_nDHB$ (pro = proline, DHB = 2,5-dihydroxybenzoic acid, n = 0, 1, 2 or 4) clusters has been studied both experimentally and computationally. Experimentally the $(pro)_nDHB$ clusters are generated in the gas phase by laser desorption and supersonic jet entrainment. The photoionization thresholds are then determined by the mass-selective measurement of both one and two-color photoionization efficiency curves. These experiments demonstrate that the ionization energies (IEs) of the $(pro)_nDHB$ clusters are substantially reduced in comparison to the IE of free DHB. Computational studies of the $(pro)_nDHB$ clusters provide insights into the mechanism of IE reduction. For the (pro)DHB system the IE reduction results from spin delocalization in the ion state of the cluster. In contrast, for the $(pro)_2DHB$ and $(pro)_4DHB$ clusters the IE reduction results from an inductive delocalization of electron density from pro to DHB in the ground state of the cluster. This latter effect, which is a result of the specific hydrogen-bonding interactions occurring in the mixed clusters, leads to IE reductions of over 1 eV. Finally, determination of the energetics of the $(pro)_2DHB$ radical cation demonstrate that the DHB-to-proline proton transfer reaction is a barrierless, exoergic process in the ion state and that energetic demands for cluster dissociation to protonated $(pro)_2$ plus a deprotonated DHB radical are substantially lower than those for cluster dissociation to $(pro)_2$ plus $DHB^{+\bullet}$. Cumulatively, these studies provide new energetic and mechanistic insights into the MALDI matrix-to-analyte proton transfer process.

Key Words:

1. MALDI-MS
2. Ionization Mechanism(s)
3. Ionization Energies
4. Clusters
5. Computational Modeling

Introduction

Over the last decade and a half matrix-assisted laser desorption / ionization (MALDI) has emerged as a powerful method for the mass spectrometric analysis of large, intact biomolecules.[1] In practice the MALDI method involves co-crystallization of the biomolecular analyte with an excess of a typically small, functionalized aromatic molecule referred to as the matrix. In the simplest terms it is generally agreed that the role of the matrix is to both assist in the desorption of the co-crystallized biomolecule and participate in biomolecule ionization via one of a number of possible mechanisms, including proton transfer. Beyond this simplistic description, however, much remains unclear as to the mechanistic details of the MALDI process.

Over the years a wide variety of mechanistic studies have been performed with the goal of elucidating various details of the MALDI mechanism and a number of recent reviews summarize much of the current thinking regarding this important technique.[2,3,4] An important distinction has been made between primary and secondary ionization processes in MALDI.[2,4] The primary ionization processes are those occurring during or shortly after the laser pulse that lead to the initial ions. The secondary ionization processes are those occurring in the ensuing desorption plume, which may be thought of as an efficient ion-molecule reactor under typical experimental conditions, that can lead to substantial modification of the composition of the plume.[4] Secondary reactions have been found to be largely under thermodynamic control, reflecting the high temperature and collision frequency of the early plume.[4] To the extent that the relevant gas-phase thermodynamic data is available, this makes secondary processes relatively straightforward to predict.

The present study is mostly concerned with the more difficult part of MALDI ionization, the primary ionization step. In previous work it has been shown that the ionization energies

(IEs) of many matrices lie above the two-photon energy of the commonly used nitrogen laser.[2,5,6] That fact is difficult to reconcile with the high efficiency of MALDI ion generation since ion formation would only result from three-photon excitation of the matrix. However, the possibility that specific matrix-analyte interactions alter the matrix IEs could not be ruled out in these studies. That this possibility must be considered is evident in the work of several researchers who have explored matrix-to-analyte proton transfer occurring in small clusters.[7,8,9,10,11,12,13,14] Several of these reports have suggested that clustering of MALDI matrices with neutral nitrogen containing molecules (e.g. amino acids, peptides, etc.) results in substantial reductions in the IE of the cluster as compared with the IE of the free MALDI matrix.[10,11,12,13,14] To date, however, no detailed studies of this effect have been reported.

In this paper, we have measured the two-photon photoionization efficiency thresholds and calculated the corresponding vertical IEs for the gas phase clusters, $(pro)_nDHB$ (pro = proline, n = 0, 1, 2 or 4, DHB = 2,5-dihydroxybenzoic acid) . We show that the IEs, which are associated with ionization from the π system of the DHB, are dramatically lowered, from 8.0475 eV in unassociated DHB to 6.96±0.02 eV in the $(pro)_4DHB$ complex. Further, we demonstrate that the IE lowering in the larger clusters is primarily due to an inductive effect, with secondary contributions from delocalization of the unpaired electron in the ion state. Finally, a key aspect of secondary ionization reactions is examined, that of protonation of the analyte. Since biomolecules are very often detected in MALDI in protonated form, this is a process that must be understood. Donation of a proton from the matrix to analyte is found to proceed without barrier in the ionized complex. The energy needed to dissociate the complex and liberate the protonated analyte is also computed.

Experimental Details

Molecular clusters of DHB and pro were generated using laser desorption and supersonic jet entrainment, similar to methods described in previous work.[11,12,13] Particular care was given to the method of sample preparation and to the introduction of the sample to the supersonic jet expansion in an effort to obtain reproducible number densities of the $(pro)_n$DHB clusters over many laser desorption events. The DHB / pro sample was made by dissolving DHB and pro in methanol in a 1:1 mass ratio. After evaporation of the methanol the resulting coarse crystals of DHB / pro were ground to a fine powder using a mortar and pestle. The powder was then deposited in a slotted sample holder and subsequently pressed to form a solid sample pellet.

An external stepper motor was used to translate the sample holder through a guide slot located below the opening of the pulsed valve, ensuring that fresh sample was always exposed to the desorption laser. Desorption was performed using the moderately focused 355 nm output from a Nd:YAG laser impinging on the sample directly in front of the valve opening. The desorption region was structured such that a large part of the adiabatic expansion and cooling occurs after mixing of the desorbed material and the carrier gas (argon, 1 bar backing pressure). The $(pro)_n$DHB cluster molecular beam was skimmed and passed into the acceleration region of a 1 m linear time-of-flight mass spectrometer, where it was intersected by the unfocussed output of a tunable dye laser system. Example $(pro)_n$DHB cluster mass spectra obtained using the approach described and at different laser wavelengths are shown in Fig. 1.

The photoionization thresholds of the $(pro)_n$DHB clusters were determined by measurement of resonant one-color 1 + 1 photoionization efficiency (PIE) curves. In these experiments a tunable, nanosecond duration, frequency doubled dye laser was used to excite the DHB chromophore in the cluster from the ground to the first electronic excited state, and subsequently to ionize the excited clusters. The laser wavelength was increased (decreasing total

ionization energy) until the ion signal from each cluster dropped to insignificant levels. The mass spectra were summed for at least 256 laser shots at each wavelength, and repeated measurement series were performed with both increasing and decreasing wavelength. The composite results of the one-color measurements are depicted in Fig. 2. In addition, two-color experiments were performed using a constant, resonant $S_1 \leftarrow S_0$ excitation wavelength with the second, ionization wavelength chosen to provide equivalent total 2-photon energies as those employed in the one-color experiments. These two-color experiments allowed potential errors resulting from non-resonant $S_1 \leftarrow S_0$ absorption to be eliminated and confirmed the PIE thresholds obtained in the one-color experiments.

Computational Details

A detailed computational study of the $(pro)_n$DHB clusters was also performed. The initial conformational search for the clusters was carried out at the force field level.[15] All geometries were subsequently fully optimized using density functional theory (DFT) level with the non-local B3LYP[16,17] functional and large basis sets[18]. Each stationary point was characterized as a true minimum by analytic frequency calculations. All calculations were performed with the programs Gaussian 98[19] and PQS[20]. Vertical IEs were calculated as the energy difference between the neutral and cationic species at the geometry of the neutral species. Because the observed IE lowering could be due to a destabilization of the neutral species or a stabilization of the ionized species, it was important to distinguish between ground and ion state effects. To differentiate between these effects, Koopmans' Theorem[21] IEs (KTIEs) were also calculated at the Hartree-Fock level. The KTIE of a molecule is essentially the negative of the energy of the highest occupied molecular orbital of the unionized species, and therefore measures ground state but not ion state effects.

Results and Discussion

Experimental IEs of the (pro)$_n$DHB (n = 0, 1, 2, 4) clusters. In Fig. 2 a comparison of the PIE curve for desorbed and entrained DHB with that obtained by using conventional molecular beam techniques, in which vaporized DHB is co-expanded with the carrier gas, demonstrates the efficacy of the entrainment adiabatic cooling process. Only a small amount of thermal broadening of the ionization threshold is observed with the entrainment source. The (pro)$_2$DHB and (pro)$_4$DHB raw data appear to indicate very similar thresholds for both species. Upon closer inspection, it is apparent that the two curves are similar in shape at the lowest 2-photon energies, but diverge at higher energies. Even the unusual resonance peak of the (pro)$_4$DHB curve is reproduced with reduced amplitude in the (pro)$_2$DHB signal. This is an indication of a common effect in such studies, fragmentation or evaporation in the ion state. In this case, a proline dimer is apparently lost. Correcting for this effect is not entirely straightforward, since the fragmentation yield vs. ion state excess energy is not known.

In Fig 2 we have made the simplest assumption: that the fragmentation yield is constant across the energy range measured. The (pro)$_4$DHB signal was scaled to fit the (pro)$_2$DHB curve at low 2-photon energies and subsequently subtracted from the (pro)$_2$DHB data. This shifts the ionization threshold about 0.05 eV upward. The correction is therefore much smaller than the difference in PIE thresholds between (pro)DHB and (pro)$_2$DHB (see Table 1).

To arrive at the cluster IEs shown in Table 1 one additional assumption was made. Since the PIE thresholds in Fig 2 all exhibit a rounded tail toward lower energy, the upper limit of the vertical IE value was established by a linear extrapolation to zero intensity of the portion of the PIE curve above the tail. The curvature of the PIE thresholds is the main source of the uncertainty in the IE values reported in Table 1, where it can be seen that the cluster IEs drop

from 8.0475 eV for DHB to 6.94-6.98 eV for $(pro)_4$DHB. The approach employed is based on the assumption that the observed tailing is due to thermal broadening and is consistent with the broadening observed for the desorbed and entrained DHB as compared to the DHB molecular beam PEI curves. It should be noted, however, that PIE thresholds may be curved for other reasons such as relaxation of the cluster geometry in either the intermediate or ion states. Regardless, the extrapolated PIE thresholds are believed to be near the vertical IEs of the $(pro)_n$DHB clusters. This conclusion is supported by the excellent agreement of the experimentally determined values with the calculated values reported below.

Calculated IEs of the $(pro)_n$DHB (n = 0, 1, 2, 4) clusters. To gauge the level of accuracy of the theoretical calculations, the vertical IE of free DHB was calculated. A value of 8.11 eV was found, in excellent agreement with the experimental value of 8.0475 eV.[5] The lowest energy conformation of DHB (Fig. 3) was used for these calculations.[22] The calculated KTIE is 8.50 eV.[23] KTIEs are typically larger than experimental vertical IEs, because charge reorganization in the cation, which will stabilize the cation and lower the IE, is neglected.

In the $(pro)_1$DHB complex (Fig. 4), the pro and DHB are bound through their carboxylic acid groups. The calculated IE (7.67 eV) agrees well with experiment (7.80-7.92eV) and is significantly lower than the IE of free DHB. However, the KTIE of 8.49 eV is essentially identical to the KTIE of free DHB (8.50 eV). Therefore, the lowering of the IE upon going from DHB to $(pro)_1$DHB is not a ground state effect, but must result from stabilization of the ionized species. The origin of this stabilization is clear. In the radical cation, an electron has been ionized from the π system of the DHB, leaving one unpaired electron on DHB. However, a Mulliken population analysis[24] of $(pro)_1DHB^{+\bullet}$ demonstrates that the spin (i.e. the "last" unpaired electron) is only 60%

localized on DHB in $(pro)_1DHB^{+\bullet}$ (and therefore 40% delocalized to pro). This delocalization from DHB to pro stabilizes the cation and lowers the IE.

The delocalization is through the carboxylic acid double hydrogen bonds between DHB and proline. DHB has an extensive π system consisting of the benzene ring, both OH groups and the carboxylic acid group. Pro also has a quasi π system consisting of the carboxylic acid group and the nitrogen lone pair. In $(pro)_1DHB$ these two π systems are coupled by the hydrogen bonds between the two carboxylic acid groups, forming an extended planar quasi π system (a least-squares plane through the DHB, the carboxylic acid group and the proline nitrogen shows a maximum deviation from planarity of 0.061 Å). This allows for delocalization of the unpaired electron of DHB to pro.

The $(pro)_nDHB$, n = 2 or 4, clusters are quite similar and will be discussed together. The most stable $(pro)_2DHB$ cluster (Fig. 5) consists of a pro dimer (through the carboxylic acid linkages), with DHB hydrogen bound to both pro nitrogens, one via the DHB carboxylic acid proton, and one via the proton on the 5-OH group. The $(pro)_4DHB$ cluster (Fig. 6) may be thought of as a dimer of pro dimers, with the pro dimers bound via N-H---N hydrogen bonds. The DHB sits in the $(pro)_4$ "pocket" and hydrogen bonds to one nitrogen on each pro dimer. Both of these clusters are strongly bound relative to free pro and DHB. The calculated binding energies for $(pro)_2DHB$ and $(pro)_4DHB$ are 110.3 kJ/mol and 197.0 kJ/mol, respectively. The calculated IE for $(pro)_2DHB$ is 7.16 eV, compared to the experimental value of 7.00-7.06 eV.[25] For $(pro)_4DHB$, the calculated IE is 6.97 eV, while the experimental value is 6.94-6.98 eV. Both calculations are in essentially perfect agreement with experiment.[26]

The mechanism of IE reduction in the $(pro)_2DHB$ and $(pro)_4DHB$ clusters is significantly different than that of the $(pro)_1DHB$ system. Unlike the $(pro)_1DHB$ cluster, the KTIEs for the

$(pro)_2DHB$ and $(pro)_4DHB$ clusters are dramatically lower when compared to free DHB. For $(pro)_2DHB$, the KTIE is 7.67 eV, while for $(pro)_4$ DHB it is 7.60 eV (recall that the KTIE of free DHB is 8.50 eV). The 0.83-0.90 eV drop in the KTIEs of these clusters relative to free DHB correlates well with the 0.9-1.1 eV drop in experimental IEs. In addition, because DHB is bound to pro via N---HO hydrogen bonds (rather than the double carboxylic acid linkage found in the $(pro)_1DHB$ cluster) the larger clusters do not form a quasi π system between pro and DHB, and therefore exhibit little delocalization of the unpaired electron. A Mulliken population analysis indicates that this electron is highly localized on DHB in both cluster ions (99% for $(pro)_2DHB^{+\bullet}$ and 85% for $(pro)_4DHB^{+\bullet}$). It follows that delocalization in the radical cation is not an important factor for the $(pro)_2DHB^{+\bullet}$ system, and is at best a secondary factor for the $(pro)_4DHB^{+\bullet}$ ion.

The KTIEs clearly show that the mechanism of IE reduction is a ground state effect i.e., the highest occupied molecular orbital of DHB is destabilized in the $(pro)_nDHB$, n = 2, 4 systems. A more detailed analysis shows that virtually all of the frontier orbitals localized on DHB are also destabilized in both complexes. Unlike the $(pro)_1DHB$ system, in which the two monomeric units are linked via two OH---O hydrogen bonds, the larger systems have pro nitrogens hydrogen bonded to DHB OH groups. The latter arrangement provides for efficient inductive donation of electron density from pro to DHB. This is clearly indicated by Natural Population Analyses[27,28] on the clusters which yield group charges on DHB of -0.12 e^- (n = 2) and -0.15 e^- (n = 4). The buildup of electron density on DHB raises the energy of all of the frontier orbitals, and therefore lowers the IE. In contrast, the group natural charge of DHB in $(pro)_1DHB$ is only -0.02 e^-.

Proton transfer in the $(pro)_2DHB$ radical cation. Two questions intimately related to the mechanism of MALDI may also be addressed using the proline/DHB system. First, what

structural rearrangements occur in the vertically ionized cluster immediately following ionization, and second, what are the thermodynamic relationships between the radical cation cluster and the various possible dissociation products. To answer these two questions we examined the energetics for cluster dissociation in the $(pro)_2$DHB cluster. We chose to investigate this species for two reasons. First, the mechanism of IP lowering in this species and the $(pro)_4$DHB cluster were essentially identical, leading us to conclude that the behavior of the ionized $(pro)_n$DHB (n=2 or 4) clusters should be analogous. Second, the smaller size of the $(pro)_2$DHB was more amenable to calculation.

Allowing the vertically ionized geometry to relax generates the structure shown in Fig. 7 in which a proton transfer from DHB to the pro_2 moiety has occurred without a barrier. Remarkably, it is the phenolic proton originally at the 5-position of DHB, rather than the carboxylic acid proton, which transfers to pro_2. This process is significantly exoergic (ΔE = 96.2 kJ/mol). To understand the origin of the unusually high acidity of the phenolic proton in the DHB radical cation, we performed a series of gas phase acidity (GA)[29] calculations on benzoic acid, phenol, *p*-hydroxybenzoic acid and *m*-hydroxybenzoic acid (ortho substituents were avoided to eliminate the complicating effects of intramolecular hydrogen bonding). The results are shown in Table 2. The radical cations of benzoic acid and phenol have almost identical GAs (830.8 and 831.8 kJ/mol, respectively). For comparison, the GAs of *neutral* benzoic acid and phenol are 1442 and 1476 kJ/mol, respectively. Thus, upon going from the neutral species to the radical cation, the phenolic proton becomes more acidic when compared to its' benzoic acid counterpart. This may be attributed to resonance stabilization of the deprotonated phenol radical. Deprotonation of the radical cation via loss of the phenolic hydrogen yields a highly resonance stabilized radical with the unpaired electron delocalized into the aromatic ring, while loss of the carboxylic acid proton leads to a structure with the unpaired electron localized on the -COO

group. This is illustrated nicely by the resonance structures of the radical cations of deprotonated benzoic acid and phenol.[30]

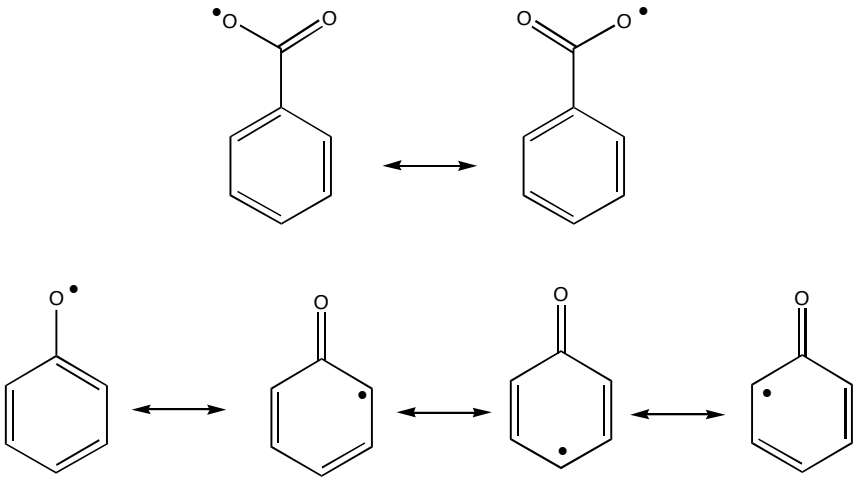

For hydroxybenzoic acid, the phenolic proton is always more acidic than the carboxylic proton. The reasons for this are clear. Consider *p*-hydroxybenzoic acid. Deprotonation at the carboxylic group yields the following resonance structures:

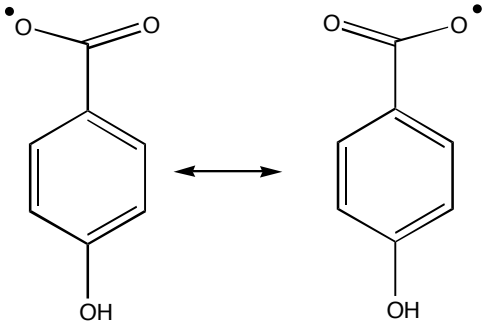

However, deprotonation at the phenol group yields the following resonance structures:[31]

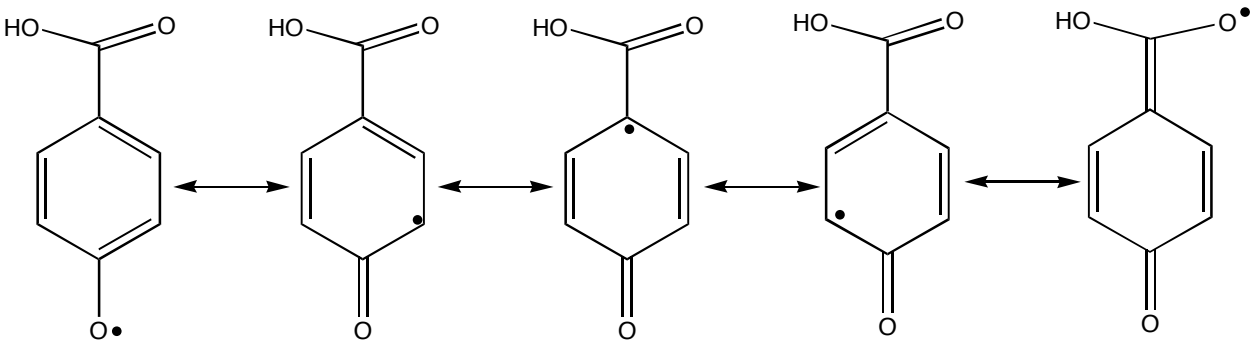

Therefore, the radical created by deprotonation at the phenol group has much greater resonance stabilization, resulting in a greater acidity.

One can imagine two possible channels for dissociation of the ionized $(pro)_2DHB$ complex: (1) dissociation to pro_2 and the DHB radical cation, $(DHB^{+\bullet})$, and (2) dissociation to protonated pro_2 (pro_2+H^+) and the deprotonated DHB radical $(DHB\text{-}H^+)^\bullet$. Fig. 8 shows the energetic relationships between these two channels and the $(pro)_2DHB$ radical cation in the initial (neutral state)and final (ion state) geometries. Dissociation from the ion state geometry to yield pro_2 and $DHB^{+\bullet}$ requires 235.2 kJ/mol (2.43 eV), whereas dissociation to yield pro_2+H^+ and $(DHB\text{-}H^+)^\bullet$ requires only 141.0 kJ/mol (1.47eV). The large excess energy required for dissociation without proton transfer is consistent with the results of recent experimental studies of clusters of DHB with the tripeptide VPL.[13] In these studies it was found that dissociation to $DHB^{+\bullet}$ and VPL was only significant when the 2 or 3 photon energy used for cluster ionization exceeded the maximum IE of the $VPL_{m>1}DHB_{n<3}$ clusters by more than 2.3 eV.

Conclusions

It is clear from the results of these studies that reductions in the IE of DHB do occur upon interaction of this MALDI matrix with the amino acid proline. For the (pro)DHB cluster the modest IE reduction is primarily the result of spin delocalization in the –COOH bridged

(pro)DHB cluster radical cation. In contrast, for the $(pro)_2$DHB and $(pro)_4$DHB clusters both the experimental and computational studies confirm that IE reductions of over 1 eV do occur as a result of N---H-O hydrogen bonding interactions between amino acid nitrogen atoms and the –COOH and meta –OH groups on the DHB. Interestingly, the large IE reductions observed for the $(pro)_2$DHB and $(pro)_4$DHB clusters are primarily the result of a ground state inductive charging of the DHB aromatic ring leading to a significant negative charge on the DHB. In addition, it is shown that matrix-to-analyte proton transfer in the ionized $(pro)_2$DHB cluster is a barrierless, exoergic process and furthermore, that the energetic demand for cluster dissociation to $(pro)_2H^+$ plus $(DHB\text{-}H^+)^\bullet$ is substantially lower than that for dissociation to pro_2 plus $DHB^{+\bullet}$.

It should be noted that the IE-reducing hydrogen-bonding interactions that occur in the $(pro)_2$DHB and $(pro)_4$DHB clusters are undoubtedly not unique to these clusters. Indeed it may be expected that these effects will occur upon the interaction of DHB with other polypeptides and proteins. A direct 1 + 1 two-photon primary ionization process should thus be considered potentially active for similar classes of matrix and analyte. This is likely not the sole primary ionization pathway, however, since the same matrix yields an equally strong total ion current when no analyte is present (and two-photon ionization is not energetically possible).

Both the influence of specific matrix-analyte interactions on matrix IEs and secondary ion state proton transfer reactions in matrix-analyte complexes clearly need to be studied more extensively. As described in our early experimental studies[32], and explored in molecular dynamics simulations[33,34] and subsequently incorporated in widely cited models[3], evidence for the involvement of these complexes is growing. Indeed, recent experimental studies specifically implicate DHB-analyte clusters as ion precursors in UV-MALDI.[35] These clusters may be the result of direct ionization of the neutral complex, as here, or may form in the plume as a result of

the interaction of a matrix ion with a neutral analyte. The barrierless reaction in the present case shows that the rate limiting aspect of analyte protonation may often be collisional dissociation of the reactive matrix-analyte complex. If so, physical characteristics of the plume will have a major effect on the ion yield.

Acknowledgements

The authors acknowledge financial support from the following sources: DSM, The Welch Foundation (Y-0743); GRK, The Welch Foundation (Y-1463); RK, ETH Internal Research Grant (0-20402-97) and the Swiss National Science Foundation (21-63558). We also thank Ms. Faten Yassin for assistance with some of the calculations and Professor Martin Pomerantz for helpful discussions.

References

1. Hillenkamp F, Karas M, Beavis R, Chait RC. *Anal. Chem.* 1991; **63:** 1193A.
2. Zenobi R, Knochenmuss R. *Mass Spectrom. Rev.* 1998; **17:** 337.
3. Karas M, Glückmann M, Schäfer J. *J. Mass Spectrom.* 2000; **35:** 1.
4. Knochenmuss R, Stortelder A, Breuker K, Zenobi R. *J. Mass Spectrom.* 2000; **35:** 1237.
5. Karbach V, Knochenmuss R. *Rapid Commun. Mass Spectrom.* 1998; **12:** 968.
6. Lin Q, Knochenmuss R. *Rapid Commun. Mass Spectrom.* 2002; **15:** 1422.
7. Krutchinski AN, Dolguine AI, Khodorkovske MA. *Anal. Chem.* 1995; **67:** 1963.
8. Meffert A, Grotemeyer J. *Eur. Mass Spectrom.* 1995; **1:** 594.
9. Meffert A, Grotemeyer J. *Ber. Bunsenges. Phys. Chem.* 1998; **102**: 459.
10. Meffert A, Grotemeyer J. *Int. J. Mass Spectrom.* 2001; **210/211:** 521.
11. Land CM, Kinsel GR. *J. Am. Soc. Mass Spectrom.* 1998; **9:** 1060.
12. Land CM, Kinsel GR. *Eur. Mass Spectrom.* 1999; **5:** 117.
13. Land CM, Kinsel GR. *J. Am. Soc. Mass Spectrom.* 2001; **12:** 726.
14. Huang Y, Russell DH. *Int. J. Mass Spectrom. Ion Proc.* 1998; **175:** 187.
15. We used the Merck Molecular Force Field (MMFF) as implemented in Spartan 5.1. MMFF: Halgren TA. *J. Comput. Chem.* 1999; **20:** 730. Spartan 5.1: Wavefunction, Inc., 18401 Von Karman Ave., Ste. 370, Irvine, CA 92612. A combination of extensive Monte Carlo simulations and geometry optimization runs starting from chemically reasonable structures was employed. The importance of pro dimers as a fundamental structural unit in the clusters was hinted at by the experimental data, since the wavelength dependent changes in the mass spectra clearly implicate fragmentation of the $(pro)_4DHB^{+\bullet}$ cluster via loss of $(pro)_2$ to form $(pro)_2DHB^{+\bullet}$. This behavior is consistent

with the dimerization of the proline molecules in the neutral $(pro)_2DHB$ and $(pro)_4DHB$ clusters. Also, the minimal signal obtained for $(pro)_3DHB^{+\bullet}$ is consistent with the apparent stability of the pro dimer in these clusters.

16. Becke AD. *J. Chem. Phys*. 1993; **98:** 5648.

17. Lee C, Yang W, Parr RG. *Phys. Rev. B*. 1988; **37:** 785.

18. We employed a hybrid basis set for geometry optimizations defined as follows: 6-31+G** for H, O and N, and 6-31G** for C. Final energetics were evaluated using the same functional with the 6-31+G** basis set on all atoms. All cationic clusters were nearly pure doublet states, with $<S^2>$ less than 0.76. For the study of proton transfer in the $(pro)_2DHB$ complex, we used the 6-31+G** basis set for all atoms.

19. Gaussian 98 (Revision A.7), Frisch MJ. *et al.*, Gaussian, Inc., Pittsburgh PA, 1998.

20. PQS version 2.2. Parallel Quantum Solutions, 2013 Green Acres Road Suite A, Fayetteville Arkansas 72762.

21. Koopmans T. *Physica*. 1933; **1:** 104.

22. Similar calculations of the ground state structure of DHB and the adiabatic IE of DHB have been reported recently (Bourcier S, Bouchonnet S, Hoppilliard Y. *Int. J. Mass Spectrom*. 2001; **210/211:** 59.).

23. The highest occupied molecular orbital of all clusters corresponds to the same π orbital on the DHB. Therefore, the KTIP measures the stabilization or destabilization of this orbital in the cluster environment.

24. Mulliken RS. *J. Chem. Phys*. 1963; **38:** 2686.

25. A second, relatively stable, conformer for the $(pro)_2DHB$ cluster was also located. This species has a pro-DHB linkage similar to that found in the $(pro)_1DHB$ cluster, with the

second pro bonded to DHB via the pro carboxylic acid group and the 5-OH group of DHB. This structure is 29 kJ/mol less stable than the low energy conformer, and has a calculated IP of 7.44 eV, in significantly poorer agreement with experiment than the lower energy structure.

26. It is likely that many closely related conformers of the $(pro)_4$DHB cluster exist. One such conformer was found by rotating the DHB such that the position of the carboxylic acid group and the 5-OH group were interchanged, followed by re-optimization of the geometry. The resultant structure is only 5.2 kJ/mol less stable than the lower energy conformer, and the calculated IP is 6.98 eV. The similarity of energies and IPs of these two conformers is not surprising, given that the number and type of hydrogen bonds are identical.

27. Carpenter E, Weinhold F. *J. Mol. Struct. (THEOCHEM)*. 1988; **169:** 41.

28. Reed AE, Curtiss LA, Weinhold F. *Chem. Rev*. 1988; **88:** 899.

29. The gas phase acidity is the ΔG for deprotonation.

30. Only resonance structures without formal charge separation are considered. Also, only one of the two Kekule structures of benzene is shown.

31. For the meta isomer, only the first four of these resonance structures are valid.

32. Kinsel GR, Gimon-Kinsel ME, Gillig K, Russell DH. *J. Mass Spectrom*. 1999; **34:** 684.

33. Zhigilei LV, Garrison BJ. *Rapid Commun. Mass Spectrom*. 1998; **12:** 1273.

34. Itina TE, Zhigilei LV, Garrison BJ. *J. Phys. Chem. B*. 2002; **106:** 303.

35. Fournier I, Brunot A, Tabet JC, Bolbach G. *Int. J. Mass Spectrom*. 2002; **213:** 203.

Table 1. Measured[a] and Calculated IEs for the $(pro)_nDHB$ Clusters.

	DHB IE (eV)	(pro)DHB IE (eV)	$(pro)_2DHB$ IE (eV)	$(pro)_4DHB$ IE (eV)
PIE threshold	8.0475 (5)	7.80-7.92	7.00-7.06	6.94-6.98
Vertical IE, calculated	8.11	7.67	7.16	6.97
Koopmans IE, calculated	8.50	8.49	7.67	7.60

[a] The minimum experimental value is the 2-photon energy at which the cluster ion signal vanishes and the maximum is the linear extrapolation from the approach to the threshold.

Table 2. Calculated Gas Phase Acidities of the Radical Cations of Simple Phenol and Benzoic Acid Derivatives.[a]

phenol	830.8
benzoic acid	831.8
p-hydroxybenzoic acid (COOH)	891.4
m-hydroxybenzoic acid (COOH)	895.7
p-hydroxybenzoic acid (OH)	816.6
m-hydroxybenzoic acid (OH)	816.1

[a] All values in kJ/mol. The group in parentheses indicates where deprotonation occurs.

Figure Captions

Figure 1. Mass spectra of $(pro)_nDHB$ clusters at various one-color two-photon energies.

Figure 2. Photoionization efficiency curves of some $(pro)_nDHB$ clusters.

Figure 3. The lowest energy conformation of DHB, as determined at the DFT level.

Figure 4. The DFT optimized geometry of the $(pro)_1DHB$ complex.

Figure 5. The DFT optimized geometry of the $(pro)_2DHB$ complex.

Figure 6. Two views of the DFT optimized geometry of the $(pro)_4DHB$ complex.

Figure 7. The optimized geometry of $(pro)_2DHB^{+\bullet}$

Figure 8. The relative energies of various species relevant to $(pro)_2DHB^{+\bullet}$ and possible dissociation fragments, in kJ/mol. Note that proton transfer from DHB to pro has already occurred in the ion state geometry of $(pro)_2DHB^{+\bullet}$.

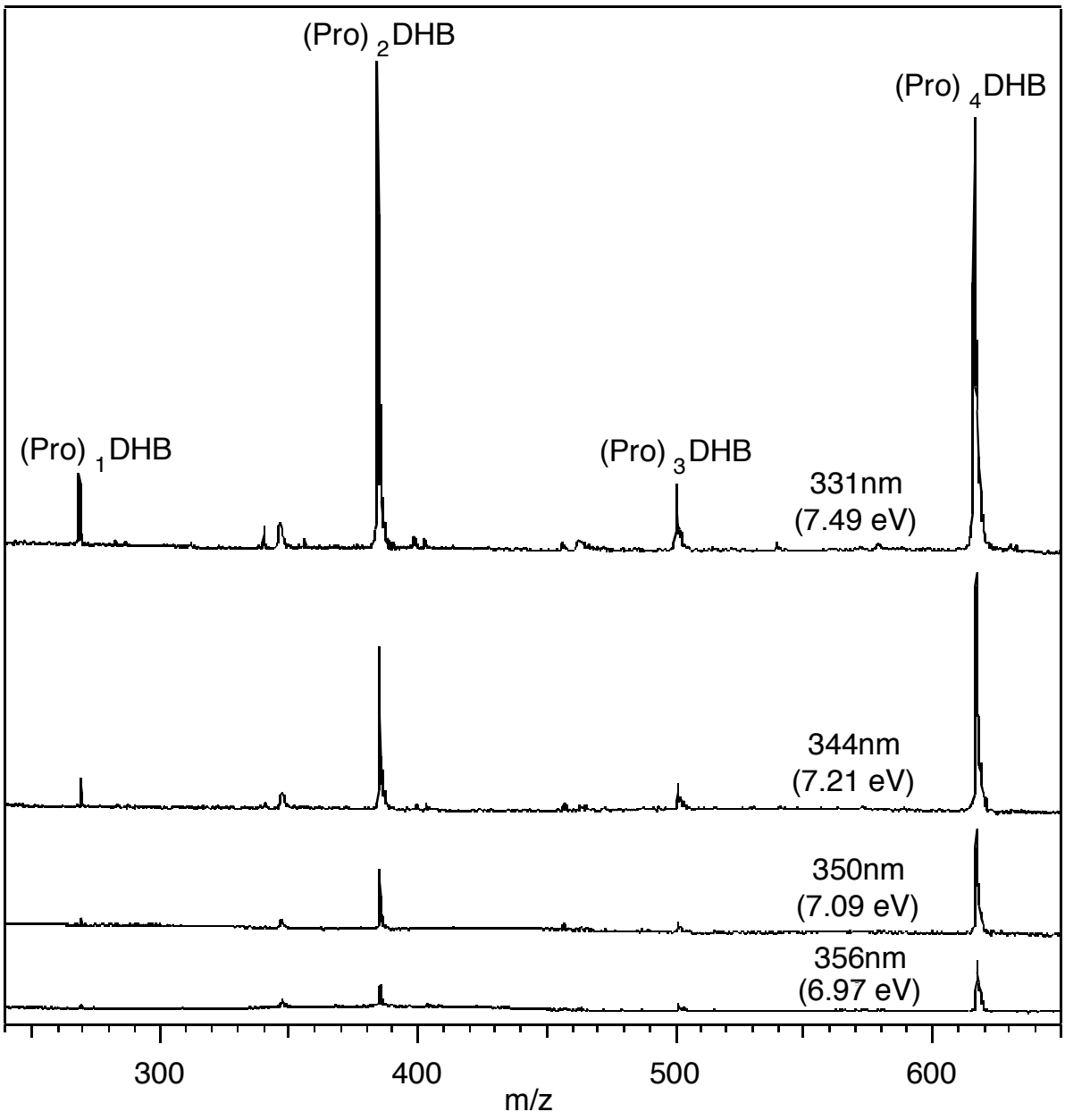
(Pro) 2DHB
(Pro) 4DHB
(Pro) 1DHB
(Pro) 3DHB
331nm
(7.49 eV)
344nm
(7.21 eV)
350nm
(7.09 eV)
356nm
(6.97 eV)
300
400
500
600
m/z

Figure 1

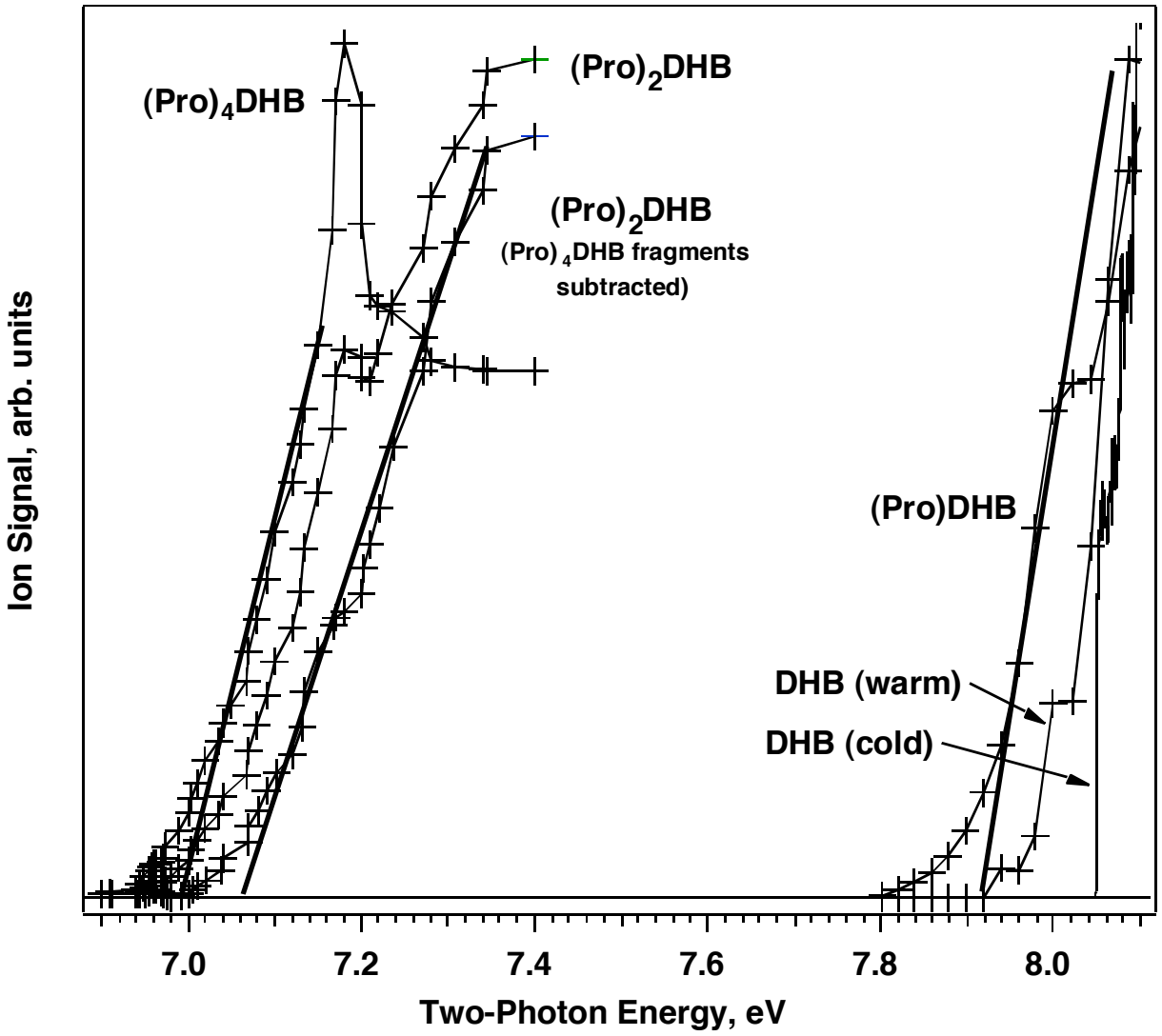
(Pro)4DHB
(Pro)2DHB
(Pro)2DHB
(Pro)4DHB fragments
subtracted)
(Pro)DHB
DHB (warm)
DHB (cold)
Ion Signal, arb. units
7.0
7.2
7.4
7.6
7.8
8.0
Two-Photon Energy, eV

Figure 2

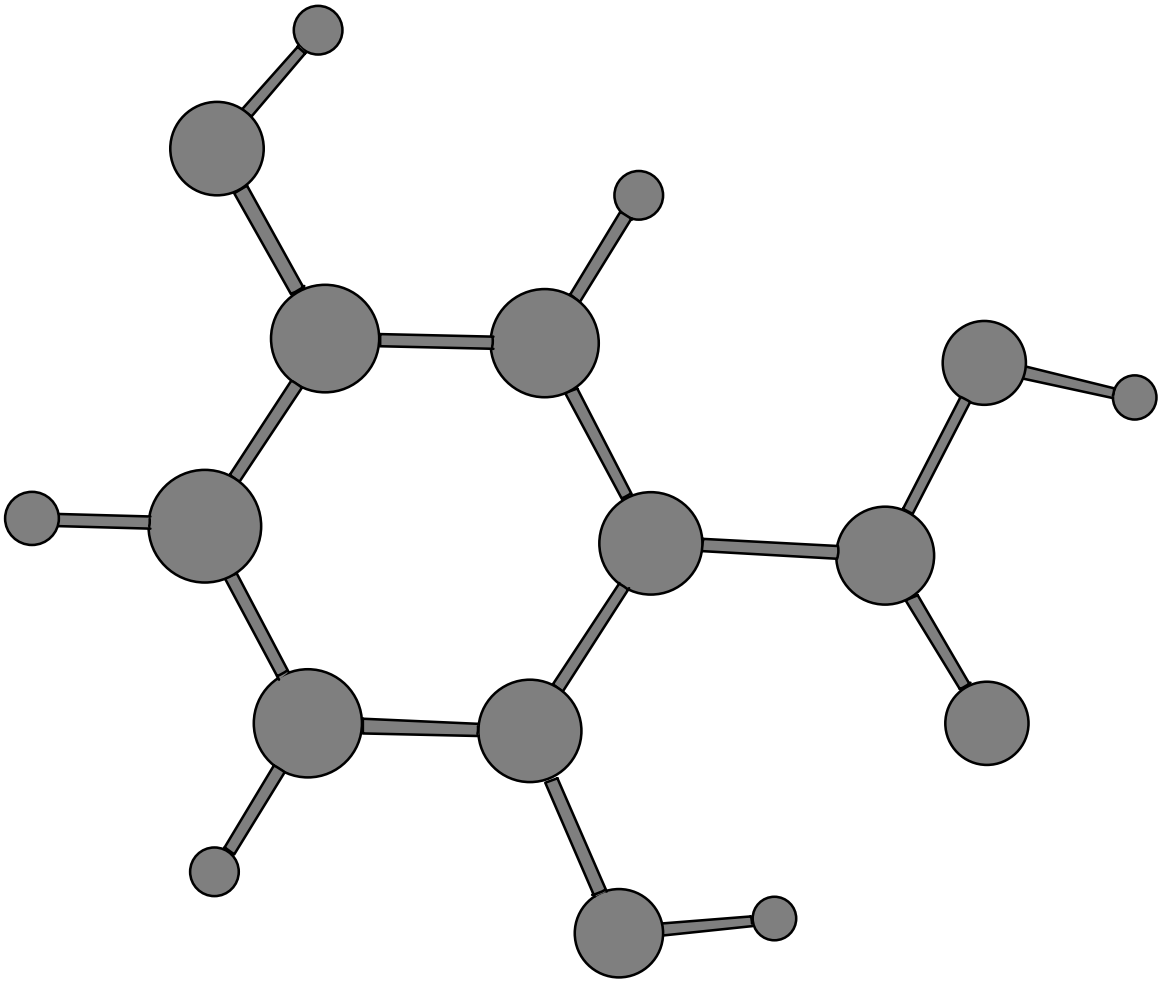

Figure 3

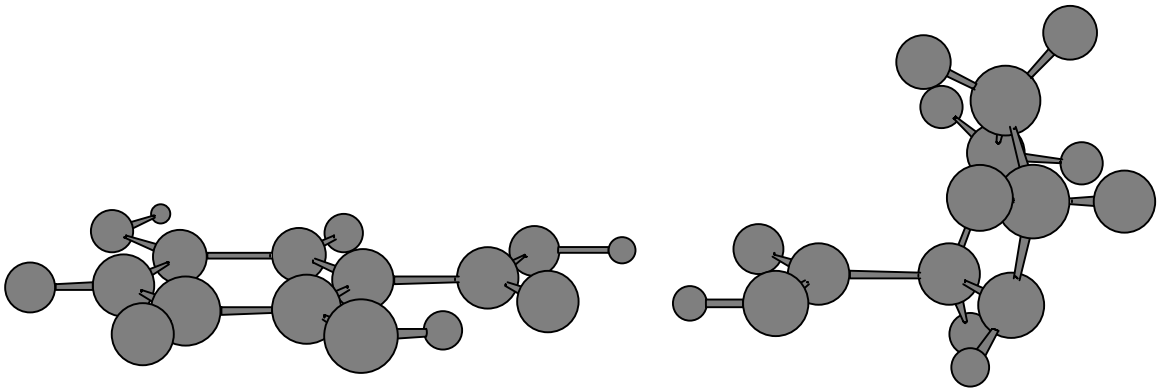

Figure 4

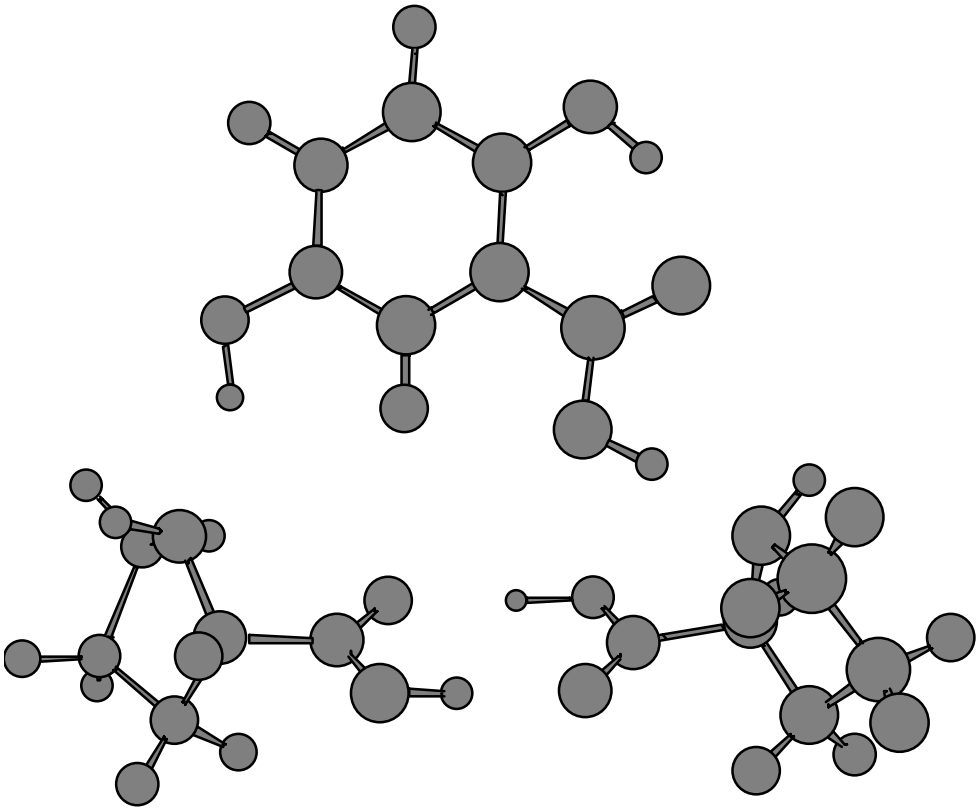

Figure 5

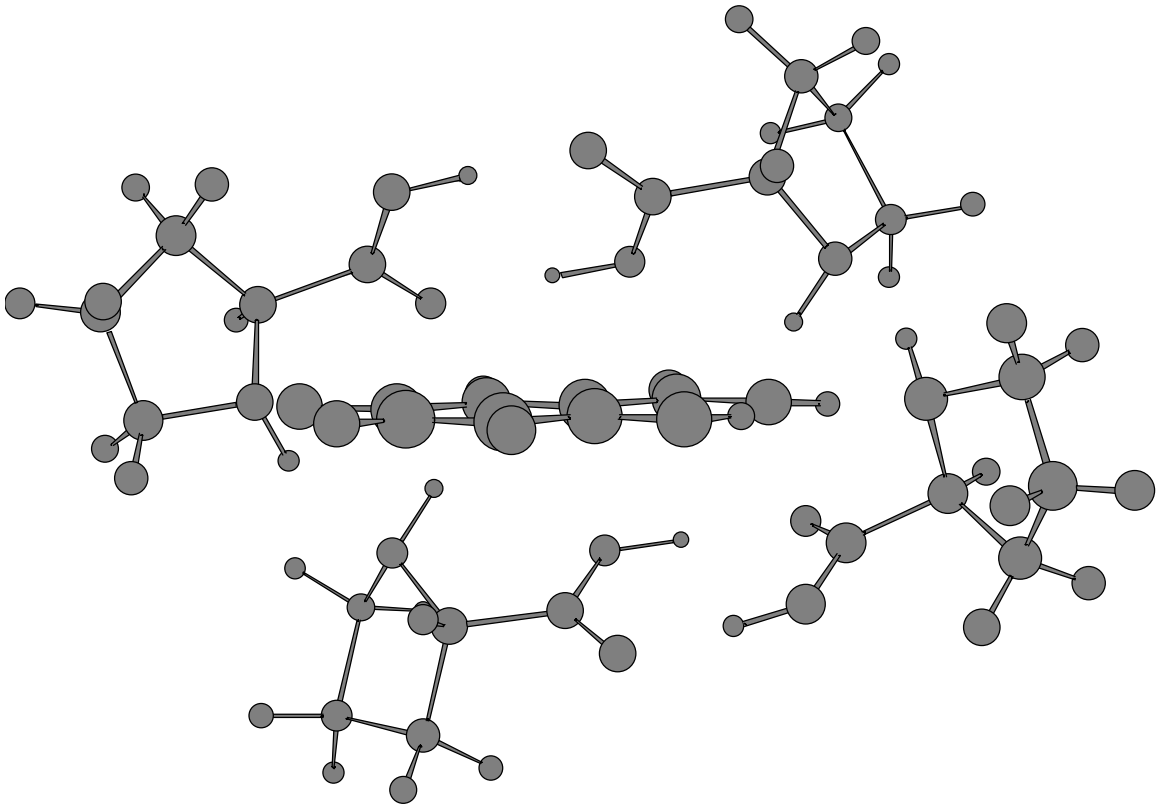

Figure 6 a

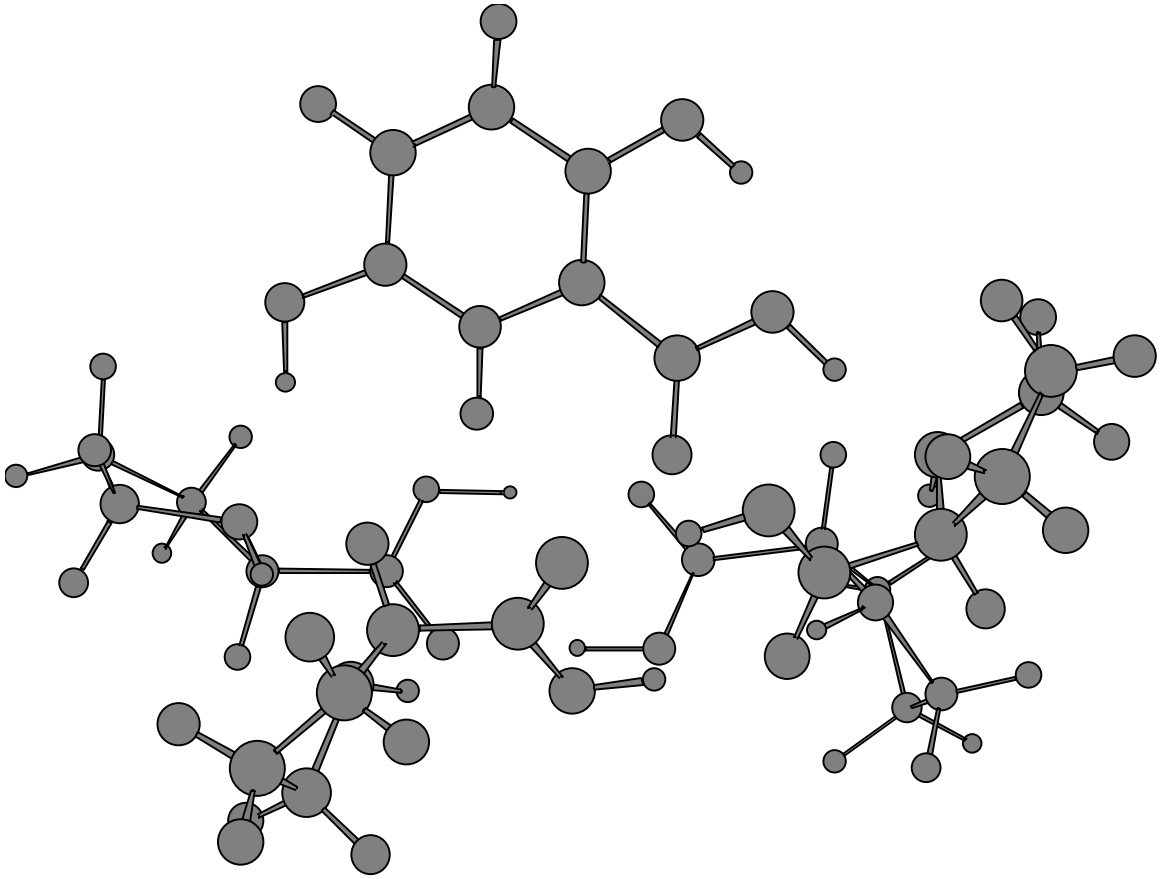

Figure 6 b

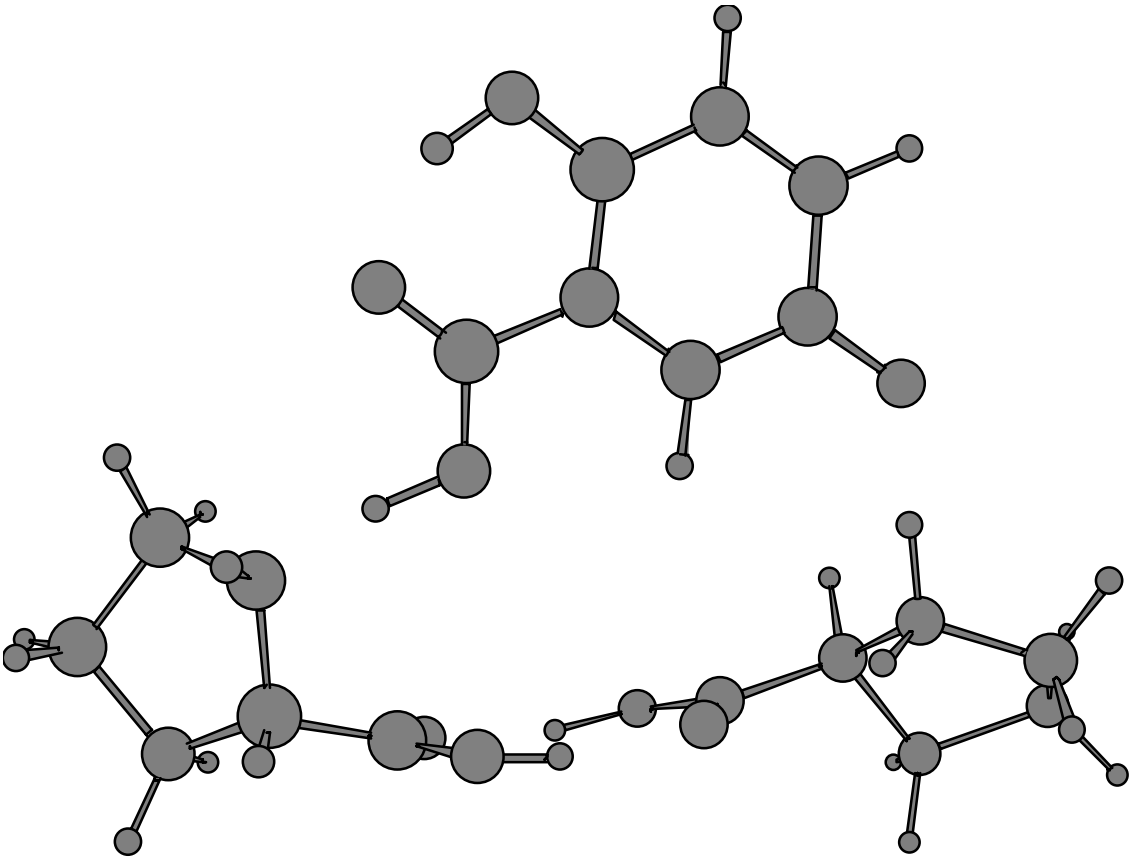

Figure 7

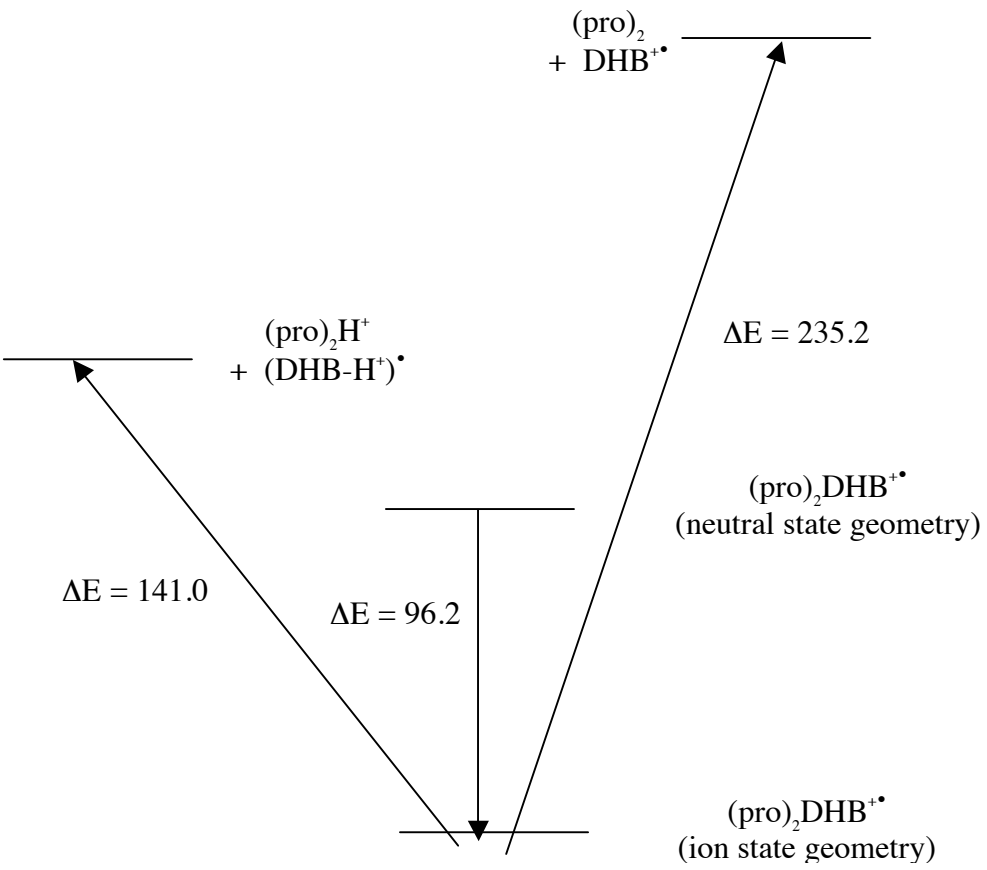
(pro)2
+ DHB+•
(pro)2H+
+ (DHB-H+)•
ΔE = 235.2
(pro)2DHB+•
(neutral state geometry)
ΔE = 141.0
ΔE = 96.2
(pro)2DHB+•
(ion state geometry)

Figure 8